DOI: 10.1002/chem.200700901

Intermediates in the Destruction of Chlorinated C_1 Hydrocarbons on La-Based Materials: Mechanistic Implications

Alwies W. A. M. van der Heijden, Maria Garcia Ramos, and Bert M. Weckhuysen*[a]

Abstract: Activity experiments using GC analysis of reactor effluent have been combined with in situ IR spectroscopy to elucidate the reaction steps in the destructive adsorption of $CHCl_3$, CH_2Cl_2, and CH_3Cl over LaOCl. The IR results show that during reaction, LaOCl is covered with carbonate, formate, and methoxy groups. The relative amount of each of these surface intermediates depends on the Cl/H ratio of the reactant. The decomposition of the surface species leads to formation of the reaction products, and is influenced by the temperature and the relative amount of Cl present on the surface. The GC results show that the activity for the destructive adsorption of H-containing chlorinated C_1 compounds decreases with increasing hydrogen content of the reactant. The acquired insight into the mechanism of destructive adsorption is crucial to the design of new catalyst materials for the efficient conversion of chlorinated hydrocarbons into nonhazardous products or reusable chemicals.

Keywords: adsorption • chlorohydrocarbons • heterogeneous catalysis • IR spectroscopy • lanthanum

Introduction

In the last few decades, the demand for products containing chlorinated hydrocarbons (CHCs), such as lubricants, heat-transfer fluids, plasticizers, and cleaning solvents, has increased.[1,2] The use of CHCs in commercial products has been greatly reduced by the introduction of alternatives that are environmentally less harmful. The current main source of chlorine waste is the so-called "lights", which is a mixture of chlorinated C_1 and C_2 hydrocarbons produced during industrial processes involving chlorine. On account of the toxic and suspected carcinogenic properties of these compounds, the emission of CHCs can cause severe damage to our environment.[3,4] Currently, incineration is the preferred method of destruction.[5–7] However, high temperatures are required to prevent the formation of toxic by-products, such as dioxins and furans. Worldwide, research efforts are being made to find cleaner and more effective routes for destroying CHCs. Alternative and cleaner destruction techniques have been investigated, such as oxidative catalysis over transition-metal oxides and noble metals.[8–11] Alkaline-earth metal oxides and lanthanide oxides convert CHCs into O-containing products, for example CO_2.[12–25] This process, known as destructive adsorption, involves exchange of the Cl atoms of the CHC with the lattice O atoms of the metal oxide. As a result, the metal oxide is partially or completely converted into the corresponding metal chloride. This process can be envisaged as: $2M_2O_3+3CCl_4\rightarrow 4MCl_3+3CO_2$ (M: metal). The use of basic oxides for the conversion of CHCs offers several advantages in comparison with other techniques. In contrast to transition-metal oxides and noble-metal catalysts, the materials possess higher stability, as no poisoning of the catalyst with Cl occurs. Besides, the cost of the solid is relatively low compared to noble-metal catalysts. Furthermore, the reaction takes place at relatively low temperatures, whereas incineration requires high temperatures.

Previous publications have reported on the destructive adsorption and catalytic destruction of CCl_4. Van der Avert et al. found that the destructive adsorption can be made catalytic by adding steam to the reaction mixture.[26,27] The chlorinated metal oxide can then exchange lattice Cl with O atoms from water, resulting in the formation of HCl. Different metal oxides were tested for this catalytic route and lanthanum proved to have the best combination of activity and stability.[26,27] Consequently, lanthanide oxide systems have been studied in great detail for the destructive adsorption of CCl_4. During reaction with CCl_4, La_2O_3 is successively converted into LaOCl and $LaCl_3$. In fact, LaOCl was

---

[a] A. W. A. M. van der Heijden, M. Garcia Ramos,
Prof. Dr. ir. B. M. Weckhuysen
Inorganic Chemistry and Catalysis Group
Department of Chemistry
Utrecht University
Sorbonnelaan 16, 3584 CA Utrecht (The Netherlands)
Fax: (+31) 302-511-027
E-mail: b.m.weckhuysen@uu.nl

found to be a more active material than La_2O_3.[28,29] Further investigations on LaOCl materials showed a link between activity and the acid–base properties of the catalyst.[30] For the destructive adsorption of CCl_4, a strong lanthanum Lewis acid site results in high activity. Since chlorine is more electronegative than oxygen, a higher chlorine content at the surface results in higher activity. However, a certain amount of oxygen is needed at the surface to enable the exchange of Cl for O atoms. As the mechanism of destructive adsorption of CCl_4 is now well understood and the active site for the reaction has been identified, our research is now focusing on the destruction of $CHCl_3$, CH_2Cl_2, and CH_3Cl.

Herein, we report a general mechanism for the destructive adsorption of chlorinated C_1 hydrocarbons and the relationship between the composition of the catalyst and the observed activity and selectivity. In situ IR spectroscopy and GC analysis were used to monitor the reaction. As a result, fundamental insight is obtained into the intermediates of destructive adsorption when applying La-based materials to convert mixtures of chlorinated C_1 compounds. This is of high relevance when destroying the "lights" in industrial waste streams.

Results and Discussion

IR spectroscopic studies: When chlorinated C_1 hydrocarbons adsorb on lanthanum oxide based materials, C−Cl bonds are broken and C−O bonds are formed resulting in chemisorption of the chlorinated C_1 compound. Both bonds are related to IR-active vibrations, and therefore IR spectroscopy enables characterization of the surface species and chemisorbed reaction intermediates. IR spectra of the gas phase and catalyst wafer were recorded separately during the reaction of LaOCl with $CHCl_3$, CH_2Cl_2, and CH_3Cl (Figures 1 and 2). Unfortunately, small fluctuations in the concentration of am-

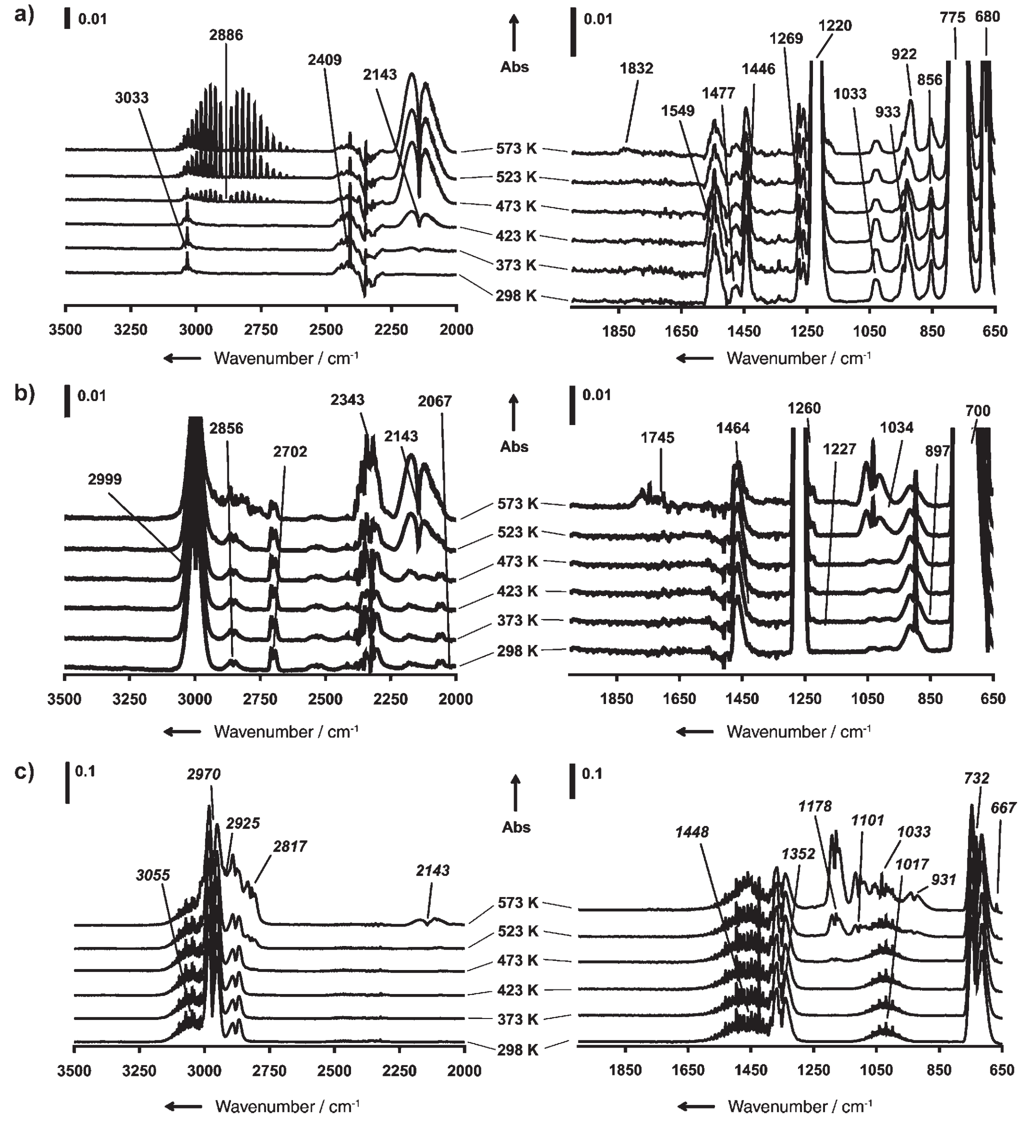

Figure 1. Gas-phase IR spectra measured during the destructive adsorption of a) $CHCl_3$, b) CH_2Cl_2, and c) CH_3Cl on LaOCl at 298, 373, 423, 473, 523, and 573 K. For comparison, a relative intensity scale is included for each spectrum.

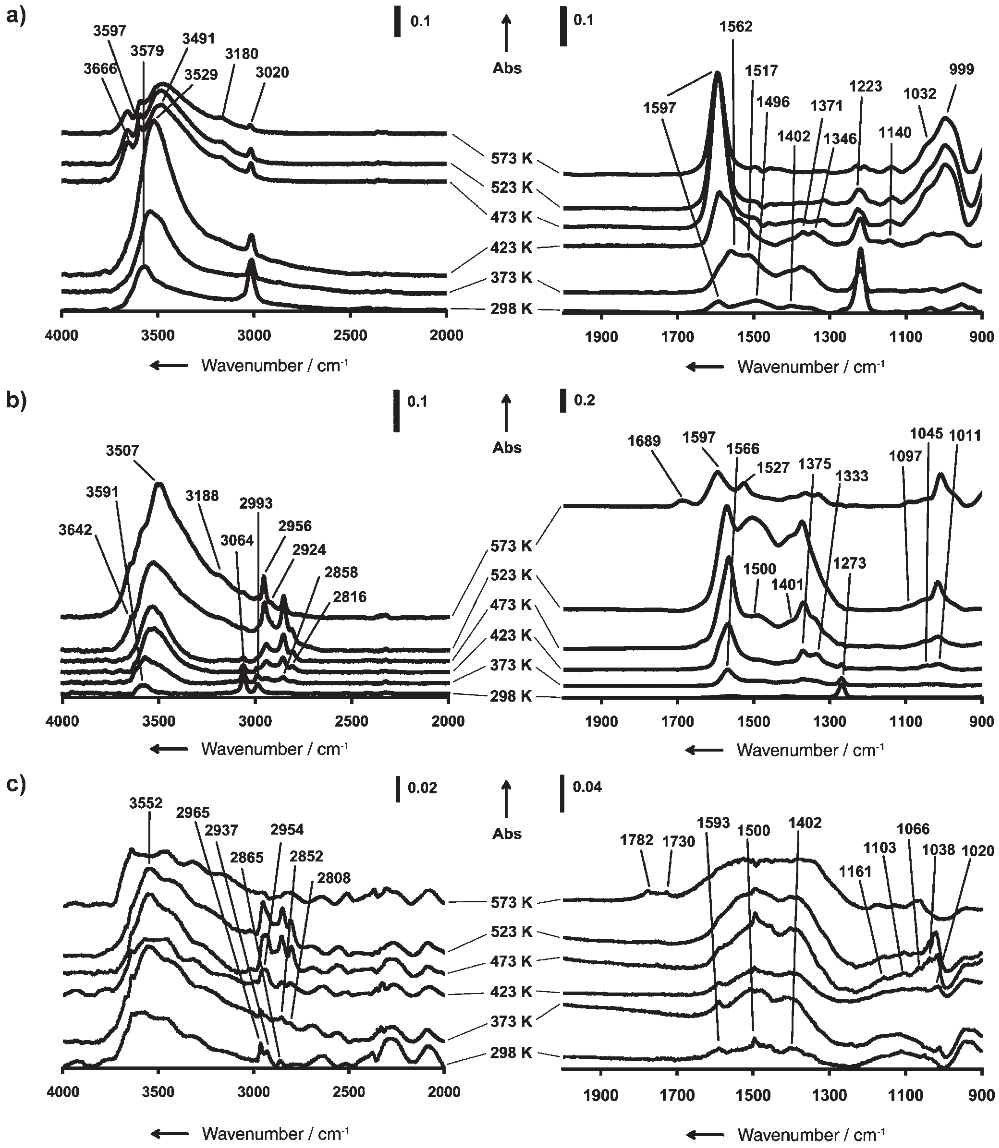

Figure 2. IR spectra of the LaOCl wafer measured during the destructive adsorption of a) $CHCl_3$, b) CH_2Cl_2, and c) CH_3Cl at 298, 373, 423, 473, 523, and 573 K. For comparison, a relative intensity scale is included for each spectrum.

bient CO_2 and H_2O prevented the accurate detection of these species as reaction products. Consequently, CO_2 and H_2O are not included in the spectra and in the discussion of the IR results.

$CHCl_3$: Several bands are observed in the gas-phase spectra at room temperature (Figure 1a). The band at 1269 cm^{-1} is indicative of CH_2Cl_2 that was present as a contaminant in the reactant.[31] The remainder of the bands are assigned to $CHCl_3$.[31] At 423 K a band arises at 2143 cm^{-1}, which is characteristic for CO.[31] The intensity of the CO band increases with increasing reaction temperature. At 473 K, the rotation–vibration pattern of HCl is observed at 2886 cm^{-1}.[31] As the temperature increases, the intensity of the HCl band also increases. A low-intensity band at 1832 cm^{-1} is visible at 573 K and is accompanied by a broadening of the band at 856 cm^{-1}. The bands are due to the formation of $COCl_2$ and the relatively low intensity indicates that a small amount is formed.[32] In addition, a band arises at 922 cm^{-1}, which can be assigned to C_2Cl_4.[31]

To elucidate the surface reaction steps of the conversion of $CHCl_3$, spectra of the wafer were also measured. In Figure 2a, each spectrum is shown after subtraction of the corresponding gas-phase spectrum and the spectrum of the wafer prior to reaction. The bands at 3020 and 1223 cm^{-1} are assigned to physisorbed $CHCl_3$. In addition, immediately after introduction of $CHCl_3$, a broad band at 3579 cm^{-1} is visible, characteristic of surface hydroxyl groups. Simultaneously with the OH bands at room temperature, bands appear at 1402, 1496, and 1597 cm^{-1}. These bands are also visible in the spectrum of LaOCl under ambient conditions and are attributed to the presence of bulk carbonate (1402 and 1496 cm^{-1}) and bidentate carbonate (1597 cm^{-1}). As a result of the high basicity of lanthanum oxide based materials, carbonates and hydroxyl groups are formed readily at room temperature by reaction with CO_2 and H_2O from air.

In a blank experiment, LaOCl was kept under static vacuum in the reaction cell to verify whether the observed bands are a result of the presence of air, or of destructive adsorption of $CHCl_3$. The intensity of the carbonate bands in the blank experiment was of the same order of magnitude as that observed in the spectrum at 298 K for the experiment with $CHCl_3$. The carbonate bands at 298 K in Figure 2a are therefore a result of residual air in the reaction cell. During the blank experiment surface hydroxyl groups were also formed, but after 4 h the intensity of the ν(OH) band was still significantly lower in comparison with the band observed after 15 min at 298 K with $CHCl_3$ in the cell. This result implies that the hydroxyl groups are formed as a result of the interaction of $CHCl_3$ with the LaOCl surface.

The abstraction of the proton from $CHCl_3$ by strong basic O sites initiates the reaction, which was also proposed by Koper et al. from experiments on the destructive adsorption of $CHCl_3$ on CaO (Scheme 1, species 1b to 2b).[33] The formation of dichlorocarbene (CCl_2) at the surface has been proven by adsorption of CCl_4 on Fe_3O_4 studied by STM.[34] Moreover, it was found that the CCl_2 fragment is mobile on the surface at 298 K. Koper et al. found from pulse experiments that $CHCl_3$ is initially converted on CaO into CO exclusively, whereas the addition of larger amounts resulted in the formation of $COCl_2$ and C_2Cl_4. Hydration of CaO led to the formation of $COCl_2$ and C_2Cl_4 after the introduction of lower amounts of $CHCl_3$. As both chlorination and hydration of the surface result in the decrease of O availability, the formation of $COCl_2$ and C_2Cl_4 is indicative of O deficiency.

The formation of C_2Cl_4 and $COCl_2$ is confirmed in the gas-phase IR spectrum for destructive adsorption of $CHCl_3$ at 573 K (Figure 1a). At 373 K, bands are visible at 1346, 1371, and 1562 cm^{-1}, which are characteristic of chemisorbed formate groups (Table 1). The intensity of the formate bands decreases in the spectrum measured at 423 K, and simultaneously CO is formed (Figure 1a). The formation of formate groups is the result of a Cl abstraction rather than proton abstraction as the initial reaction step. Initially, COHCl, an intermediate similar to $COCl_2$, is formed after exchange of two Cl atoms for an O atom (Scheme 1, species 1a to 2a). This intermediate is known to thermally disso-

Table 1. Measured vibrational frequencies and mode assignment of methoxy and formate groups after adsorption of CH_3OH and HCOOH, respectively, on LaOCl at room temperature after evacuation.

CH_3OH on LaOCl [cm^{-1}]	Methoxy mode	HCOOH on LaOCl [cm^{-1}]	Formate mode
1017	ν(CO) three-fold	1261	$\nu(OCO)_s$ monodentate
1043	ν(CO) bridged	1348	$\nu(OCO)_s$ bidentate
1062	ν(CO) bridged	1375	$\nu(OCO)_s$ bidentate
1101	ν(CO) on top	1400	δ(CH)
1460	$\delta(CH_3)$	1556	$\nu(OCO)_{as}$ bidentate
2794	$\nu_s(CH_3)$	1607	$\nu(OCO)_{as}$ bidentate
2852	$\nu_s(CH_3)$ three-fold	1689	$\nu(OCO)_{as}$ monodentate
2873	$\nu_s(CH_3)$	2859	ν(CH)
2926	$\nu_{as}(CH_3)$		
2953	$\nu_{as}(CH_3)$ three-fold		

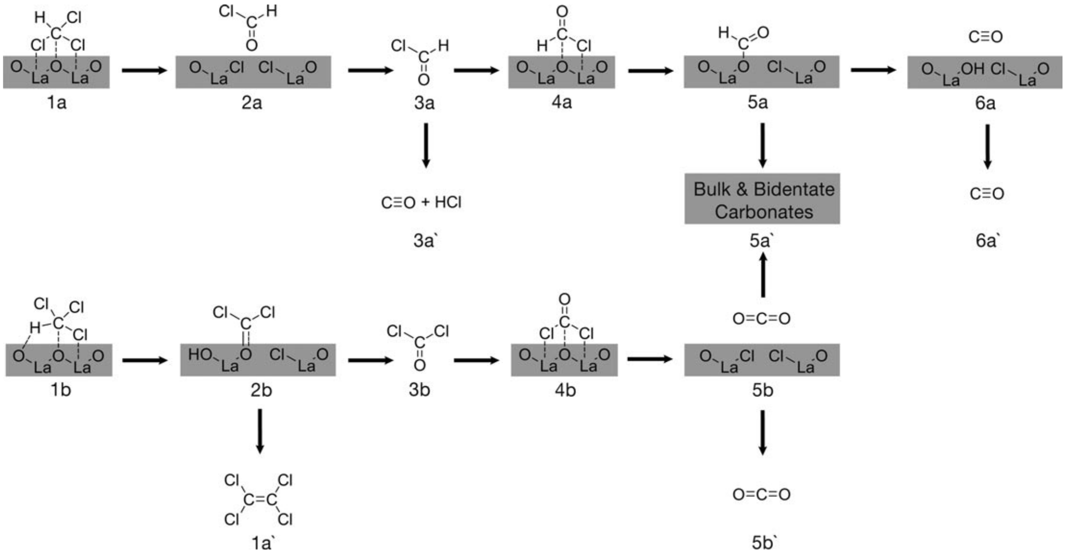

Scheme 1. Proposed reaction scheme for the destructive adsorption of $CHCl_3$ on LaOCl. To illustrate the difference between adsorbed and gas-phase species, the catalyst surface is highlighted gray.

ciate into CO and HCl (Scheme 1, species 3a to 3a′). However, when COHCl is formed at the surface, rapid readsorption is favorable, resulting in the formation of formate groups (Scheme 1, species 4a to 5a). During the increase of temperature from 298 to 423 K, the OH band at 3579 cm^{-1} also increases in intensity and shifts to 3529 cm^{-1}. The broadening and perturbation of the OH band can be explained by the interaction between OH groups and $CHCl_3$.[35]

At 473 K, the formate bands disappear and the intensity of the OH bands decreases. Moreover, three distinct maxima are visible in the ν(OH) region and a low-intensity band appears at 3180 cm^{-1}, which may be the result of hydrogen bonding between chloroform and surface hydroxyl groups. The three OH bands have previously been linked to the occurrence of different phases in lanthanum oxide powders, on the basis of XRD.[36] The bands at 3491, 3597, and 3666 cm^{-1} are assigned to LaOOH, $La(OH)_3$, and isolated LaOH, respectively.[36] The different bands are related to the degree of hydration of the sample. Initially, through proton abstraction the surface becomes saturated with OH groups and at higher chlorination degree, the OH groups react with Cl to form HCl and regenerate basic O sites. The thermal dissociation of COHCl may be more favorable at 473 K than the readsorption and consecutive formation of formate groups, as bands related to formate groups are not found in the spectrum. An alternative interpretation is that formate groups are formed which immediately dissociate into CO and surface hydroxyl groups. The decrease of the formate bands parallels the increase of the carbonate band at 1597 cm^{-1}. This result implies that the formate groups convert into bidentate carbonates (Scheme 1, species 5a to 5a′).[37]

Above 473 K, the intensity of the carbonate band at 1597 cm^{-1} decreases, which leads to CO_2 formation. As previously mentioned, however, CO_2 could not be detected due to experimental limitations. The bands at 999 and 1032 cm^{-1} are assigned to La–O vibrations. The broadness of the bands is most likely due to the rearrangement of the LaOCl structure as a result of chlorination of the catalytic surface. The band at 1140 cm^{-1} appears simultaneously with bidentate carbonate; however, no reference was found with respect to this band.

CH_2Cl_2: Bands that are all assigned to CH_2Cl_2 are observed at room temperature in the gas-phase spectra (Figure 1b).[31] At 423 K, a small shoulder arises at 1227 cm^{-1}, which can be assigned to $CHCl_3$.[31] At 473 K, CO is formed and the intensity of the CO band increases as the temperature increases. At 573 K, several bands arise at 1034 and 1745 cm^{-1}. In addition, bands are visible between 2700 and 3000 cm^{-1}. The bands at 1034 and 1745 cm^{-1} are characteristic of methanol and formaldehyde, respectively.[31] The pattern of bands in the 2700–3000 cm^{-1} region confirms the formation of CH_2O and CH_3OH.[31] The bands may in addition be indicative of HCl formation.[31]

The spectra of the catalyst, measured during the destructive adsorption of CH_2Cl_2, are shown in Figure 2b. At 298 K, bands are observed at 3064, 2993, and 1273 cm^{-1}, assigned to physisorbed CH_2Cl_2. Also, a low-intensity hydroxyl band is observed at 3590 cm^{-1}, indicating proton abstraction similar to the destructive adsorption of $CHCl_3$ (Scheme 2, species 1b to 2b). The recombination of CHCl to $C_2H_2Cl_2$ is not observed at high temperature, however. Apparently, the surface reaction involving CHCl is limited to lattice O extraction resulting in the formation of COHCl. As the temperature increases, the hydroxyl band broadens and at 573 K, three maxima are visible at 3507, 3591, and 3642 cm^{-1}. This is similar to the hydroxyl bands observed during the $CHCl_3$ experiment (Figure 2a). Even though no products are observed in the gas phase below 523 K, the wafer spectra show bands at 1566, 1375, 1336, and 2858 cm^{-1} at 373 K, indicating the formation of formate groups. This finding can be explained by the previously discussed consecutive readsorption and formation of formate groups from COHCl (Scheme 2, species 4b to 5b).

At 473 K, a broad set of bands is present at 1600–1300 cm^{-1}, which increases in intensity at 523 K. The broad bands between the two maxima at 1566 and 1375 cm^{-1} are assigned to bulk carbonates. At 423 K and higher tempera-

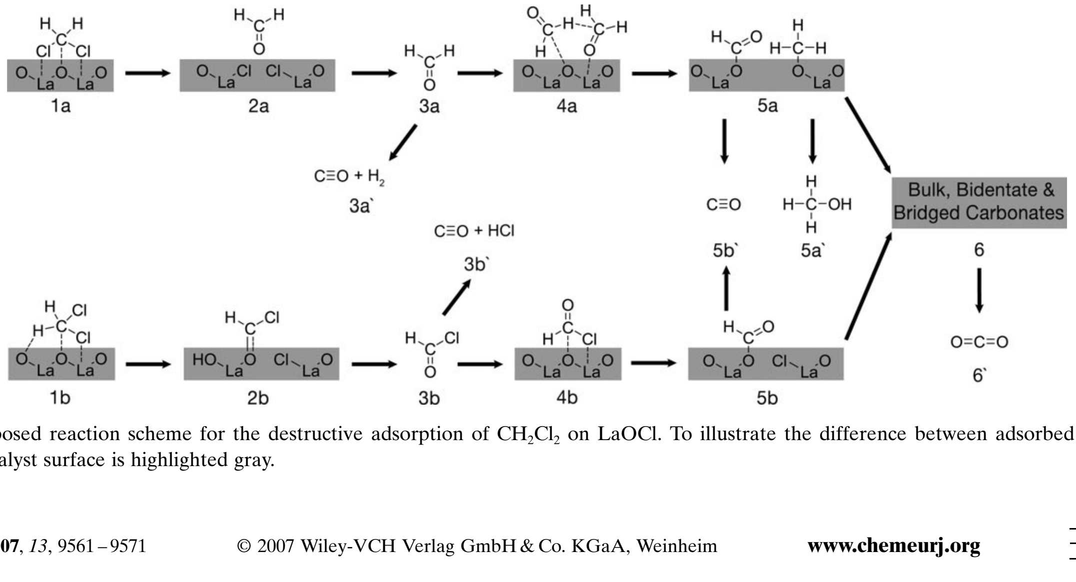

Scheme 2. Proposed reaction scheme for the destructive adsorption of CH_2Cl_2 on LaOCl. To illustrate the difference between adsorbed and gas-phase species, the catalyst surface is highlighted gray.

tures, bands are also present around 1011 and 2800–3100 cm^{-1} as a result of methoxy group formation. In previous IR experiments of methanol probing on LaOCl, different types of methoxy species have been identified based on the vibrational frequencies in the low wavenumber region (Table 1).[30] The bands observed at 1097, 1045, and 1011 cm^{-1} have been assigned to on-top, bridged, and threefold methoxy species, respectively. The methoxy species are predominantly in the threefold adsorbed state and are stable up to 573 K. The intensity of the bands at 2956 and 2858 cm^{-1} in the ν(CH) region parallels the intensity of the ν(CO) band of threefold adsorbed methoxy species. The decrease in intensity at 573 K of the band at 2858 cm^{-1} is caused by the overlap between the ν(CH) bands of formate and methoxy groups, as the formate species dissociate at 573 K. In addition to threefold methoxy species, a relatively low concentration of bridged and on-top adsorbed methoxy species is formed at the surface. Similar to the reaction with $CHCl_3$, a reaction pathway initiated by Cl abstraction may explain the formation of methoxy species. Analogous to $CHCl_3$, CH_2Cl_2 produces CH_2O after Cl removal (Scheme 2, species 1a to 2a). CH_2O is known to form dioxymethylene (O_2CH_2) and polyoxymethylene species on the surface of ionic solids, which can convert further into formate and methoxy groups.[37] However, the bands characteristic of dioxymethylene and polyoxymethylene are not observed in the spectra. Moreover, the formation of dioxymethylene requires reduction of a metal site, which is highly unlikely in the case of lanthanum.[38] On the other hand, it has been shown recently that even though La^{3+} is unable to change oxidation state, oxidation of OCl is possible.[39,40] A more likely explanation, however, is that formaldehyde reacts via a Cannizzaro-like reaction to form methoxy and formate groups (Scheme 2, species 4a to 5a)).

At 523 K, CH_3OH is formed in the gas phase. The formation of CH_3OH is linked to the increased concentration of methoxy species and hydroxyl groups at the surface. As a result, basic O sites are regenerated by CH_3OH desorption (Scheme 2). The fact that formaldehyde is observed in the gas-phase spectrum at 573 K indicates that readsorption is becoming less favorable, or that more CH_2O is formed at the surface (Scheme 2). At 573 K, bands are visible at 1689, 1597, 1527, and 1333 cm^{-1}. The band at 1689 cm^{-1} is ascribed to monodentate formate (Table 1), which means that compared to the $CHCl_3$ experiment, the formate groups remain on the surface up to higher temperatures. Therefore, temperature is not the only factor influencing dissociation. Chlorination is highly probable as an additional parameter. The bands at 1597, 1523, and 1333 cm^{-1} are assigned to carbonates remaining on the surface after dissociation of bulk carbonates. The bands at 1523 and 1333 cm^{-1} have previously been assigned to polycarbonates.[30]

CH_3Cl: For CH_3Cl on LaOCl at room temperature, the observed bands are all assigned to gas-phase CH_3Cl (Figure 1c). At 523 K, a strong band arises at 1178 cm^{-1} assigned to dimethyl ether. At 573 K, other bands indicative of dimethyl ether arise at 931, 1101, 2817, and 2925 cm^{-1}. A band is also observed at 1033 cm^{-1} as a result of methanol formation. Moreover, gas-phase C≡O at 2143 cm^{-1} is visible in the spectrum at 573 K.

During the experiment with CH_3Cl on LaOCl, bands assigned to physisorbed CH_3Cl are observed at 2965, 2937, and 2865 cm^{-1} (Figure 2c). The intensity of the bands of the surface species is significantly lower than those for the experiments with $CHCl_3$ and CH_2Cl_2, making the spectra rather noisy after subtraction. At room temperature, the ν(OH) band is visible at 3552 cm^{-1}. The intensity of this band is relatively constant throughout the experiment. This result indicates that hydrogen abstraction is not favorable in the case of CH_3Cl (Scheme 3, species 1b to 2b). At 423 K, the previously assigned bands of methoxy groups are ob-

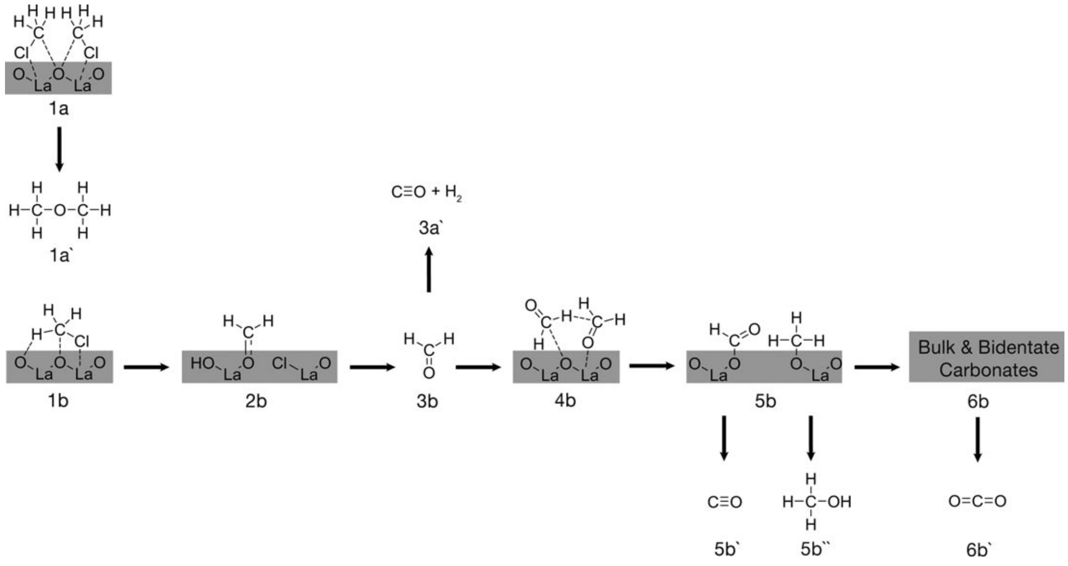

Scheme 3. Proposed reaction scheme for the destructive adsorption of CH_3Cl on LaOCl. To illustrate the difference between adsorbed and gas-phase species, the catalyst surface is highlighted gray.

served at 2954, 2852, and 2808 cm^{-1}. Broad bands are also observed in the low-wavenumber region, confirming the presence of methoxy species. The position of the band at 1020 cm^{-1} is indicative of threefold adsorbed methoxy species (Table 1). The bands at 1038, 1066, and 1103 cm^{-1} show that a relatively small amount of twofold and on-top adsorbed methoxy groups is also present at the surface. The formation of methoxy groups is accompanied by gas-phase dimethyl ether.

Two possible pathways can lead to the formation of dimethyl ether. 1) Recombination of two surface methoxy species, resulting in the regeneration of an O site. However, due to the low intensity of the methoxy bands compared to the experiment with CH_2Cl_2 on LaOCl, it appears unlikely that dimethyl ether is not formed for CH_2Cl_2. 2) A more probable pathway is the exchange of two Cl atoms from two CH_3Cl molecules for one O atom (Scheme 3, species 1a to 1a′). The CH_3Cl molecule is relatively small compared to the molecules containing more of the large Cl atoms. Therefore, the conversion of CH_3Cl into dimethyl ether is able to occur without the formation of large amounts of surface species.

At 573 K, the methoxy groups dissociate simultaneously with the formation of methanol, as was observed for the destructive adsorption of CH_2Cl_2. In addition to methoxy species, broad bands are visible at 1700–1200 cm^{-1}. These bands are similar in position and intensity for the carbonate bands that are observed for the experiments at room temperature with $CHCl_3$ and CH_2Cl_2 (Figure 2a, b). These bands were ascribed to residual air in the vacuum cell and, consequently, the formation of carbonates. The intensity of the carbonates is relatively constant in all spectra. However, at 573 K the carbonate band is broader and two low-intensity bands arise at 1782 and 1730 cm^{-1}. No reference has been found for the assignment of these bands. The broadening of the carbonate bands at 573 K may indicate the formation of formate groups. The dissociation of formate groups would consequently explain the gaseous CO that is observed at 573 K (Figure 1c).

GC activity experiments: To evaluate activity and selectivity, gas-flow experiments were performed. The region in the chromatogram where $COCl_2$ is observed contains other peaks, and therefore $COCl_2$ is difficult to detect. As a result, both the assignment and the quantification of $COCl_2$ may be susceptible to a rather large error. Therefore, $COCl_2$ has been omitted from the GC results, as it is generally formed together with CO_2. Another point of discussion is the fact that CH_3Cl and CH_3OH are co-eluting. Fortunately, the IR results complement the GC results. In the IR experiments, the formation of CH_3OH was observed, whereas the formation of CH_3Cl was not observed. The product formed during the GC experiments is therefore assigned to CH_3OH. This also means that the formation of CH_3OH could not be confirmed during the GC experiments with CH_3Cl, and consequently the conversion of this reaction is actually higher than experimentally determined.

To enable comparison of selectivity, the reactions were performed on LaOCl at 673 K. The overall conversion is shown in Figure 3. It is defined as the sum of the flow concentrations of the C-containing products divided by the sum of the flow concentrations of the reactant and the C-containing products, multiplied by 100%. The overall conversion at 673 K shows the following trend: the conversion by destructive adsorption of CH_xCl_{4-x} decreases as x increases. A trend is observed in the conversion as a function of time. Initially, the conversion is relatively high. This may not seem the case for CH_3Cl; nevertheless, because of the coelution of CH_3Cl and CH_3OH, the conversion is likely to be significantly higher than that measured by GC analysis. After some time a sharp decrease in conversion was observed. The decrease in activity is caused by the complete chlorination of the catalyst surface. Once the surface is fully chlorinated, the reaction becomes controlled by the diffusion of lattice O atoms to the surface and of lattice Cl atoms to the bulk.

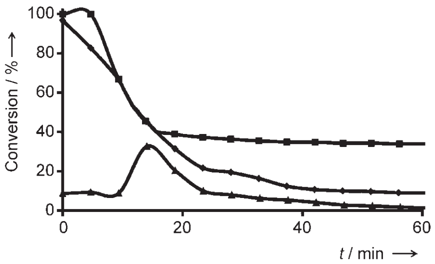

Figure 3. Overall conversion for the destructive adsorption of 6–7 vol% of $CHCl_3$ (■), CH_2Cl_2 (◆), and CH_3Cl (▲) in He on LaOCl at 673 K as a function of time.

In Figure 4, the conversion of the products is shown as a function of time for the destructive adsorption of $CHCl_3$, CH_2Cl_2, and CH_3Cl on LaOCl at 673 K. The conversion was defined as the flow concentration of a product divided by the sum of the flow concentrations of the reactant and the products, multiplied by 100%. As the reaction time increases, the surface becomes more chlorinated. Therefore, the timescale can be translated into a chemical parameter, namely, surface chlorination. The conversion curves have similar shapes: an increase, followed by a maximum value, ending in a decrease. The maximum conversion indicates that a certain degree of chlorination increases conversion. This finding is in agreement with previous experiments with CCl_4 on LaOCl, in which higher intrinsic activity was observed for a more chlorinated surface.[30] An increase in chlorination leads to stronger Lewis acid sites, which are important for the initial reaction step. Once a C–Cl bond has been broken, basic O sites are needed to stabilize the remaining fragment and to convert it into O-containing products. Therefore, an optimum combination of strong Lewis acid sites with sufficient basic O sites exists, which is controlled by the degree of surface chlorination. In the experiments on LaOCl, a maximum was not observed in some cases. The degree of chlorination of the surface has probably exceeded the optimum value. Therefore, the measurements only show the decrease in conversion following the maximum.

In all experiments, the formation of CO_2 follows the formation of other products, such as CO, CH_3OH, and CH_4. Also, the maximum conversion of CO_2 is observed later in the reaction as the H content of the reactant increases. This finding indicates that the chlorination of the surface results in the formation of CO_2. Either it promotes the formation of CO_2 as a reaction product, or carbonates are formed in an earlier stage of the reaction and desorb as CO_2 as a result of surface chlorination.

General discussion: The results of the IR analysis are summarized in Table 2. Even though different products are formed in each reaction, the reaction pathways described in Schemes 1–3 can be summarized by a general reaction scheme (Scheme 4). Two initial pathways are proposed for the destructive adsorption of the chlorinated C_1 series, that is, CCl_4, $CHCl_3$, CH_2Cl_2, and CH_3Cl. The first reaction pathway is known from the destructive adsorption of CCl_4 and is similar for the other chlorinated C_1 hydrocarbons. Two Cl atoms of the reactant are exchanged for a lattice O atom, which leads to the formation of a gas-phase intermediate, namely COH_xCl_{2-x}. In the case of CH_3Cl, another reaction may occur which resembles this pathway, as this molecule possesses only one Cl atom. Two CH_3Cl molecules both donate one Cl atom and an O atom is exchanged in return. As a result, $(CH_3)_2O$ is formed as a gas-phase product. For the destructive adsorption of CCl_4, it was found previously that an optimum combination of Lewis acidity/basicity exists for the active sites.[30] The C−Cl bond becomes elongated when the Cl atom is attracted by a La^{III} Lewis acid site, resulting in the breaking of the C−Cl bond and the formation of a La−Cl bond. The basic O sites are necessary to stabilize the remaining CCl_3 fragment and enable the conversion of CCl_4 into CO_2. The strength of the Lewis acid site therefore is a key factor for activity and this is also applicable to the other chlorinated C_1 hydrocarbons.

The second pathway results in the formation of an adsorbed $CH_{x-1}Cl_{3-x}$ fragment after removal of H and Cl atoms from the reactant (Scheme 4). Clearly, CCl_4 is unable to react via this reaction pathway due to the absence of H atoms. However, for the other chlorinated C_1 species the O site is able to abstract a H atom. A hydroxyl group is formed as a result of

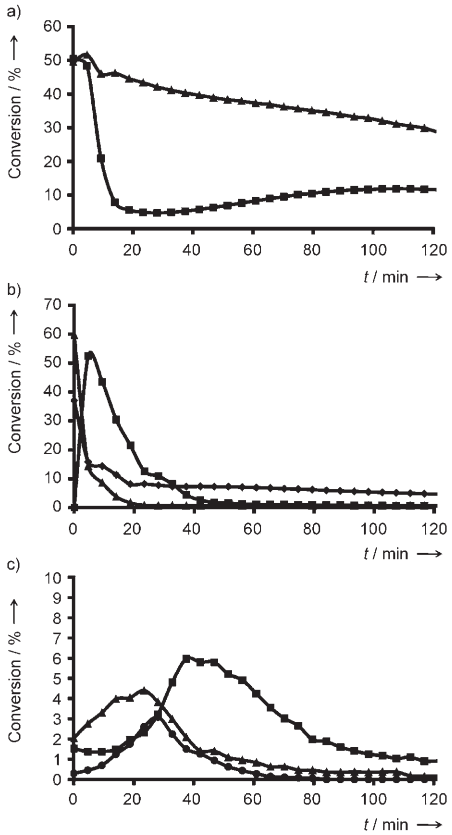

Figure 4. Conversion into each product for the destructive adsorption of $CHCl_3$, CH_2Cl_2, and CH_3Cl on LaOCl (A–C, respectively) at 673 K as a function of time. The symbols in the graphs refer to the products: CO (▲), CO_2 (■), CH_3OH (◆), and CH_4 (●).

Table 2. Overview of gas-phase and surface species detected on LaOCl with IR spectroscopy for the destructive adsorption of $CHCl_3$, CH_2Cl_2, and CH_3Cl at 298, 373, 423, 473, 523, and 573 K.

	$CHCl_3$		CH_2Cl_2		CH_3Cl	
T [K]	Surface species	Gas-phase species	Surface species	Gas-phase species	Surface species	Gas-phase species
298	hydroxyl formed	–	hydroxyl formed	–	–	–
373	formate formed	CO	formate formed	–	–	–
423	carbonate formed formate dissociated	CO	methoxy formed	–	methoxy formed	–
473	hydroxyl dissociated	CO HCl	carbonate formed formate dissociated	CO	–	–
523	carbonate dissociated	CO HCl	–	CO CH_3OH	–	$(CH_3)_2O$
573	–	CO HCl $COCl_2$ C_2Cl_4	carbonate dissociated	CO CH_3OH CH_2O	formate formed methoxy dissociated	$(CH_3)_2O$ CH_3OH CO

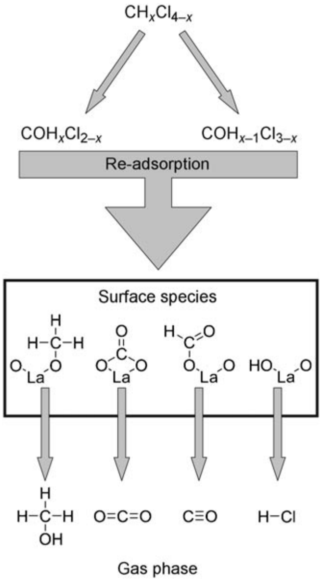

Scheme 4. Proposed general reaction scheme for the destructive adsorption of CH_xCl_{4-x} on LaOCl.

the removal of the H atom, and the Cl atom forms a bond with the La atom. Based on these results, it is not possible to determine whether the formation of the hydroxyl group precedes or follows the formation of the La−Cl bond. Nevertheless, the strength of the basic O atom directly influences the initial step of the reaction pathway. The $CH_{x-1}Cl_{3-x}$ fragment is able to migrate across the surface and remove a lattice O atom to form the gas-phase intermediate $COH_{x-1}Cl_{3-x}$. The removed O atom is not replaced by another anion and this would result in an overall positive charge on the catalyst material. However, La_2O_3-based materials are able to incorporate additional O atoms and reconstruct the catalytic surface.[41] Moreover, carbonates on the catalyst surface can change coordination to compensate for the loss of O atoms. This means that removal of H/Cl from the chlorinated C_1 compounds is dependent on the number of additional O atoms that are incorporated into the material and the amount and type of carbonates present on the catalytic surface.

Two initial pathways result in the formation of two similar intermediate products (Scheme 4). The rapid readsorption of the two intermediates, COH_xCl_{2-x} and $COH_{x-1}Cl_{3-x}$, results in the formation of hydroxyl, formate, carbonate, or methoxy groups. The surface species formed can further interconvert or dissociate into gas-phase products, depending on the degree of chlorination of the surface and the reaction temperature. $COCl_2$ is converted into CO_2 after readsorption, which may readsorb again resulting in carbonate formation. In the case of COHCl, a formate group is formed when readsorption occurs. COH_2 is readsorbed via a Cannizzaro-like reaction leading to the formation of methoxy and formate groups. In some cases, the intermediates are observed in the gas-phase spectra, that is, CH_2O and $COCl_2$ for CH_2Cl_2 and $CHCl_3$, respectively.

Constant-temperature experiments show that the conversion of H-containing chlorinated C_1 hydrocarbons decreases as the H content of the reactant increases. This trend can be explained by the change in polarization in the bonds of the CH_xCl_{4-x} molecule. The polarization of the reactant molecule is linked to the electronegativities (ENs) of the atoms, that is, C, Cl, and H with Pauling EN values of 2.55, 3.16, and 2.20, respectively. The difference in EN between the C atom and the Cl atom results in a polarization between the central atom and the substituents. As the EN of the H atom is relatively the same as that for the C atom, a C−H bond is less polarized than the C−Cl bond. Even though the direction of polarization of the C−H bond is opposite to that of the C−Cl bond, the influence of the C−H bond on the polarization of the molecule is negligible. According to the proposed reaction scheme, the initial steps involve the lengthening and consecutive breaking of the C−H bond and/or C−Cl bond. Loss of polarization as a result of decreasing Cl content stabilizes the reactant molecule, and hence reduces the susceptibility to H or Cl abstraction, resulting in lower activity. In addition to the reactant, the chlorination of the catalyst is also found to be of influence on the conversion. After a certain reaction time, a maximum conversion is reached. This shows that a specific degree of chlorination represents the optimum combination of Lewis acidity and basicity.

IR studies on the destructive adsorption of the H-containing chlorinated C_1 series revealed different products and surface species. In general, a higher H content of the reactant results in more hydrogenated reaction products. The surface species follow the same trend. The GC experiments at constant temperature show that CO_2 is formed after an initial period of chlorination. The conversion into CO_2 parallels the trend in activity for the reactants; the time of maximum CO_2 conversion is longer as the reactant becomes more hydrogenated. The IR experiments showed that carbonates are formed in all reactions discussed here. Therefore, it is concluded that carbonates are retained on the surface of the catalyst as long as sufficient O atoms are available. As the surface becomes chlorinated, CO_2 is released from the surface. The exclusive formation of CH_3OH from CH_2Cl_2 was observed on LaOCl. This illustrates how the chlorination degree of the surface influences the selectivity.

The two proposed reaction pathways based on the IR results yield different products for each reactant. A sharp decrease in the conversion into CO_2 and CO is observed for $CHCl_3$ and CH_2Cl_2, respectively. These are products resulting from the proposed pathway proceeding via H/Cl abstraction. Since the surface is O rich at the beginning of the experiment, abstraction by the Lewis basic site is favorable. As the catalyst surface becomes more chlorinated, the material becomes less basic. This results in a decreased conversion of CO_2 and CO for the experiment with $CHCl_3$ and CH_2Cl_2, respectively. The second pathway is also dependent on the availability of O atoms to enable the exchange of two Cl atoms for one O atom between the reactant and the catalytic material. However, the strength of the basic O site is not of direct influence as it is in the H/Cl abstraction pathway. This finding explains why a more gradual decrease in conversion is observed for the formation of CO and CH_3OH in the experiments with $CHCl_3$ and CH_2Cl_2, respectively.

Conclusion

For the destructive adsorption of $CHCl_3$, CH_2Cl_2, and CH_3Cl on La_2O_3 and LaOCl, two reaction pathways are established that lead to the formation of gas-phase intermediates (Scheme 4). It was found that a basic O site is able to abstract an H atom from the gas-phase molecule, which is a new aspect of destructive adsorption in comparison to the previous experiments with CCl_4. The intermediates can rapidly readsorb on the catalyst surface and form surface species. The surface species can interconvert and/or dissociate into gas-phase products. The dissociation of the surface species is dependent on the reaction temperature and the degree of surface chlorination.

With respect to activity, the same result is found as for the catalytic destruction of the same compounds found by van der Avert et al.[42] As the number of hydrogen atoms in the molecule increases, the initial temperature of reaction increases. Conversion of the chlorinated C_1 species at constant temperature decreases with increasing number of hydrogen atoms. This trend is a result of the decreasing polarization of the bonds in the chlorinated C_1 molecule as a consequence of more hydrogen atoms. The H and Cl abstraction that initiates the reaction is therefore less favorable with increasing H content. A second factor that influences conversion is the degree of chlorination of the surface. An optimum degree of surface chlorination exists, which translates to an optimal combination of Lewis acidic and basic surface sites. Therefore, control of the degree of chlorination of the surface is important when steam is added to the system to make the reaction catalytic.

The selectivity for the destructive adsorption of H-containing C_1 compounds is largely dependent on the reactant. This implies that the relative concentrations of the reactant will directly influence the product distribution when mixtures of chlorinated C_1 hydrocarbons are converted. To use the catalytic conversion of chlorinated C_1 hydrocarbons for the production of reusable chemicals, the selectivity has to be directed towards products containing C–H bonds, such as CH_3OH, $(CH_3)_2O$, and CH_2O. Also, the formation of CO, $COCl_2$, CO_2, and C_2Cl_4 needs to be minimized. A way to tune the reaction towards more desirable products may be the combination of waste streams with a hydrogen- and carbon-rich source. Surface chlorination is, in view of the proposed reaction scheme, of direct influence on the selectivity. A catalyst with ample O atoms promotes the reaction pathway involving H/Cl removal. The removal of H atoms results in less hydrogenated, and hence less desirable, surface intermediates and gas-phase products. Surface chlorination also inhibits the formation of carbonates, which reduces the formation of CO_2. Therefore, a chlorinated catalyst is more selective than, for example, pure La_2O_3. This is important when applying steam to make the reaction catalytic, because the degree of chlorination of the steady-state catalyst can be tuned for optimal conversion.

Experimental Section

Materials: LaOCl was prepared by a precipitation process using $LaCl_3{\cdot}7H_2O$ (Acros Organics, 99.99%) as precursor and NH_4OH solution.[23] The obtained gel $(La(OH)_2Cl)$ was filtered, washed, dried at 393 K, and calcined at 823 K in pure N_2 for 6 h. The details of these materials have been extensively discussed in a previous publication, therefore in this study only the main conclusions are reported.[30] LaOCl, prepared by a sol–gel reaction, is characterized by a surface area of 36 $m^2 g^{-1}$ and a pore volume of 0.3 $mL g^{-1}$. The synthesized material mainly consists of LaOCl crystallites embedded in an amorphous phase. Moreover, the prepared LaOCl contains bulk lanthanum carbonate.

IR spectroscopy with in situ temperature-programmed reaction: Due to interference by the bands of bulk carbonates on La_2O_3 with the adsorbed species, only LaOCl was used for the IR measurements. A quartz cell was employed, and all IR spectra were recorded using a Perkin Elmer 2000 spectrometer with a resolution of 4 cm^{-1}. LaOCl was pressed into self-supporting wafers (2 cm^2), and activated in situ prior to the IR measurements in dynamic vacuum at 823 K for 30 min. After pretreatment, the reactant (50 mbar) was introduced into the cell, which was then closed. The reactant was equilibrated with the sample at room temperature and, subsequently, spectra of the solid and the gas phase were recorded. The temperature of the sample was raised to 573 K in steps of 50 K. Spectra were recorded after each step. Spectra were also obtained for the adsorption of HCOOH (50 mbar) and CH_3OH (50 mbar) on LaOCl to use as a reference for the assignment of formate and methoxy groups, respectively.

Activity: Activity measurements for the destructive adsorption of CCl_4, $CHCl_3$, CH_2Cl_2, and CH_3Cl were performed in a tubular fixed-bed quartz reactor. The catalyst bed consisted of La_2O_3 or LaOCl (1.0 g) pressed in a sieve fraction (150–500 μm), and pretreated in a He flow (10 $mL min^{-1}$) at 823 K. The flow was regulated by Brooks 0–100-mL automatic mass-flow controllers. The reactant flow was generated by bubbling He through a bubbler containing the CHC in question for 30 min and out through a vent. To correct the different concentrations as a result of the vapor pressures of the CHCs, a second helium flow line was used to dilute all materials to the desired concentration. Once stabilized, the flow was led over the reactor bed of LaOCl. The reactions were performed at a constant temperature of 673 K. The flow was stabilized as described above and led over the pretreated reactor bed at 673 K. The composition of the reaction mixture was analyzed with time by a Siemens Maxum Edition 2 gas chromatograph with a sampling time of 240 s.

Acknowledgements

This work was supported by the National Research School Combination Catalysis (NRSCC) and an NWO-CW VICI Grant. We would like to thank M. Daturi (University of Caen, France) and A. Mens (Utrecht University) for their contribution to the design of the IR vacuum setup used in these experiments. We also thank T. Visser for his input regarding the IR results.

---

[1] Euro Chlor, "Chlorine Industry Review", to be found under http://www.eurochlor.org/reviews, **2007**.

[2] R. Bartsch, C. L. Curlin, T. F. Florkiewicz, B. Lüke, H.-R. Minz, T. Navin, R. Scannell, P. Schmittinger, E. Zelfel, *Chlorine: Principles and Industrial Practice*, VCH, Weinheim, **2000**.

[3] E. Browning, *Toxicity and Metabolism of Industrial Solvents*, Elsevier, New York, **1965**.
[4] R. J. Norstrom, M. Simon, D. C. G. Muir, R. E. Schweinsburg, *Environ. Sci. Technol.* **1988**, *22*, 1063–1071.
[5] A. Fullana, J. A. Conesa, R. Font, S. Sidhu, *Environ. Sci. Technol.* **2004**, *38*, 2953–2958.
[6] S. L. Huang, L. D. Pfefferle, *Environ. Sci. Technol.* **1989**, *23*, 1085–1091.
[7] J. Erb, *Environ. Prog.* **1993**, *12*, 243–245.
[8] S. C. Petrosius, R. S. Drago, *J. Chem. Soc. Chem. Commun.* **1992**, *4*, 344–345.
[9] J. M. Toledo, J. Corella, A. Sanz, *Environ. Prog.* **2001**, *20*, 167–174.
[10] S. Chatterjee, H. L. Greene, *J. Catal.* **1991**, *130*, 76–85.
[11] S. C. Petrosius, R. S. Drago, V. Young, G. C. Grunewald, *J. Am. Chem. Soc.* **1993**, *115*, 6131–6137.
[12] K. J. Klabunde, A. Khaleel, D. Park, *High Temp. Mater. Sci.* **1995**, *33*, 99–106.
[13] K. J. Klabunde, J. Stark, O. Koper, C. Mohs, D. Park, S. Decker, Y. Jiang, I. Lagadic, D. Zhang, *J. Phys. Chem.* **1996**, *100*, 12142–12153.
[14] O. Koper, Y. X. Li, K. J. Klabunde, *Chem. Mater.* **1993**, *5*, 500–505.
[15] P. D. Hooker, K. J. Klabunde, *Environ. Sci. Technol.* **1994**, *28*, 1243–1247.
[16] O. Koper, E. A. Wovchko, J. A. Glass, J. T. Yates, K. J. Klabunde, *Langmuir* **1995**, *11*, 2054–2059.
[17] O. Koper, I. Lagadic, K. J. Klabunde, *Chem. Mater.* **1997**, *9*, 838–848.
[18] B. M. Weckhuysen, G. Mestl, M. P. Rosynek, T. R. Krawietz, J. F. Haw, J. H. Lunsford, *J. Phys. Chem. B* **1998**, *102*, 3773–3778.
[19] B. M. Weckhuysen, M. P. Rosynek, J. H. Lunsford, *Phys. Chem. Chem. Phys.* **1999**, *1*, 3157–3162.
[20] Y. C. Chien, H. P. Wang, Y. W. Yang, *Environ. Sci. Technol.* **2001**, *35*, 3259–3262.
[21] Y. C. Chien, H. P. Wang, *J. Electron Spectrosc. Relat. Phenom.* **2005**, *144*, 315–318.
[22] T. Tamai, K. Inazu, K. Aika, *Chem. Lett.* **2003**, *32*, 436–437.
[23] T. Tamai, K. Inazu, K. Aika, *Bull. Chem. Soc. Jpn.* **2004**, *77*, 1239–1247.
[24] G. H. Liu, J. L. Wang, Y. F. Zhu, X. R. Zhang, *Phys. Chem. Chem. Phys.* **2004**, *6*, 985–991.
[25] G. H. Liu, Y. F. Zhu, X. R. Zhang, B. Q. Xu, *Anal. Chem.* **2002**, *74*, 6279–6284.
[26] P. van der Avert, B. M. Weckhuysen, *Angew. Chem.* **2002**, *114*, 4924–4926; *Angew. Chem. Int. Ed.* **2002**, *41*, 4730–4732.
[27] P. van der Avert, S. G. Podkolzin, O. Manoilova, H. de Winne, B. M. Weckhuysen, *Chem. Eur. J.* **2004**, *10*, 1637–1646.
[28] S. G. Podkolzin, O. V. Manoilova, B. M. Weckhuysen, *J. Phys. Chem. B* **2005**, *109*, 11634–11642.
[29] O. V. Manoilova, S. G. Podkolzin, B. Tope, J. Lercher, E. E. Stangland, J. M. Goupil, B. M. Weckhuysen, *J. Phys. Chem. B* **2004**, *108*, 15770–15781.
[30] A. W. A. M. van der Heijden, V. Bellière, L. Espinosa Alonso, M. Daturi, O. V. Manoilova, B. M. Weckhuysen, *J. Phys. Chem. B* **2005**, *109*, 23993–24001.
[31] C. J. Pouchet, *Aldrich Library of FT-IR Spectra: Vapor Phase, Vol. 3*, Aldrich Chemical Co., Milwaukee, **1989**.
[32] S.-K. Joung, T. Amemiya, M. Murabayashi, R. Cai, K. Itoh, *Surf. Sci.* **2005**, *598*, 174–184.
[33] K. Adib, N. Camillone III, J. P. Fitts, K. T. Rim, G. W. Flynn, S. A. Joyce, R. M. Osgood, Jr., *Surf. Sci.* **2002**, *497*, 127–138.
[34] R. S. Cutting, C. A. Muryn, G. Thornton, D. J. Vaughan, *Geochim. Cosmochim. Acta* **2006**, *70*, 3593–3612.
[35] H. Viqué, P. Quintard, T. Merle-Méjean, V. Lorenzelli, *J. Eur. Ceram. Soc.* **1998**, *18*, 305–309.
[36] B. Klingenberg, M. A. Vannice, *Chem. Mater.* **1996**, *8*, 2755–2768.
[37] G. Busca, G. Lamotte, J.-C. Lavalley, V. Lorenzelli, *J. Am. Chem. Soc.* **1987**, *109*, 5197–5202.
[38] C. Li, K. Domen, K. Maruya, T. Onishi, *J. Catal.* **1990**, *125*, 445–455.
[39] E. Peringer, S. G. Podkolzin, M. E. Jones, R. Olindo, J. A. Lercher, *Top. Catal.* **2006**, *38*, 211–220.
[40] S. G. Podkolzin, E. E. Stangland, M. E. Jones, E. Peringer, J. A. Lercher, *J. Am. Chem. Soc.* **2007**, *129*, 2569–2576.
[41] M. Alfredsson, C. R. A. Catlow, A. Paulidou, R. M. Nix, *Chem. Commun.* **2002**, *38*, 2128–2129.
[42] P. van der Avert, B. M. Weckhuysen, *Phys. Chem. Chem. Phys.* **2004**, *6*, 5256–5262.

Received: June 14, 2007